Quantitative Assessment of Intrinsic Carbonic Anhydrase Activity and the Capacity for Bicarbonate Oxidation in Photosystem II†

Warwick Hillier,*,‡ Iain McConnell,‡ Murray R. Badger,‡ Alain Boussac,§ Vyacheslav V. Klimov,|| G. Charles Dismukes,⊥ and Tom Wydrzynski‡

Research School of Biological Sciences, The Australian National University, Canberra, ACT 0200, Australia, Service de Bioénergétique, DBJC, URA CNRS 2096, CEA Saclay, 91191 Gif sur Yvette, France, Institute of Basic Biological Problems, Russian Academy of Sciences, Puschino, Moscow Region, 142290 Russia, and Hoyt Laboratory, Department of Chemistry, Princeton University, Princeton, New Jersey 08544

Received September 16, 2005; Revised Manuscript Received December 21, 2005

ABSTRACT: On the basis of equilibrium isotopic distribution experiments using ^{18}O-labeled water, it is generally accepted that water is the sole substrate for O_2 production by photosystem II (PSII). Nevertheless, recent studies indicating a direct interaction between bicarbonate and the donor side of PSII have been used to hypothesize that bicarbonate may have been a physiologically important substrate for O_2 production during the evolution of PSII [Dismukes, G. C., Klimov, V. V., Baranov, S. V., Kozlov, Y. N., DasGupta, J., and Tyryshikin, A. (2001) *Proc. Natl. Acad. Sci. U.S.A. 98*, 2170−2175]. To test out this hypothesis and to determine whether contemporary oxygenic organisms have the capacity to oxidize bicarbonate, we employed special rapid-mixing isotopic experiments using $^{18}O/^{13}C$-labeled bicarbonate to quantify the inherent carbonic anhydrase activity in PSII samples and the potential flux of oxygen from bicarbonate into the photosynthetically produced O_2. The measurements were made on PSII samples prepared from spinach, *Thermosynechococcus elongatus*, and *Arthrospira maxima*. For the latter organism, a strain was used that grows naturally in an alkaline, high (bi)carbonate soda lake in Africa. The results reveal that bicarbonate is not the substrate for O_2 production in these contemporary oxygenic photoautotrophs when assayed under single turnover conditions.

The accumulation and maintenance of molecular O_2 in the Earth's atmosphere are largely the result of oxygenic photosynthesis and have been one of the critical determinants in the evolution of life on the planet. Photosynthetic O_2 production is catalyzed by the unique photosystem II (PSII)[1] chlorophyll (Chl)/protein complex that had an evolutionary origin more than 2.5 billion years ago (*1*−*3*). Despite this distant heritage, the protein composition of the PSII reaction center and inorganic cofactors required for the O_2 producing chemistry appear to be largely conserved throughout all contemporary oxygenic species, from the eukaryotic higher plants and algae to the prokaryotic cyanobacteria. No related protein families or protein variants have been identified that are capable of photosynthetic O_2 production. Consequently, the evolution of this seemingly unique enzyme has been the subject of much speculation (*4*, *5*).

Considerable information is now available concerning the structure and function of PSII, particularly from the recent X-ray crystallographic studies of a cyanobacterial PSII at 3.2−3.6 Å atomic resolution (*6*−*8*). The catalytic site for O_2 production in PSII, designated as the oxygen evolving complex (OEC), consists of an inorganic core of four oxo-bridged manganese ions and one calcium ion (the Mn_4O_X-Ca_1 cluster), a special redox-active tyrosine residue (termed Y_Z), and the associated amino acids of the protein supra-structure. It has been established from mass spectrometric measurements that the O_2 produced during oxygenic photosynthesis undergoes a rapid ligand exchange with water (*9*).

To oxidize water to molecular O_2 without producing highly reactive oxygen radical intermediates, four electrons need to be extracted simultaneously from two water molecules, i.e.,

$$2H_2O \xrightarrow{4h\nu} O_2 + 4H^+ + 4e^-$$

The Gibbs free energy driving this reaction comes from the visible light energy absorbed by PSII. The bulk of the Chl *a* pigments[2] that are bound throughout the PSII complex collect the light energy and transfer it in the form of

† Support for this work was provided by a grant from the Human Frontiers Science Program Organization (RGP0029/2002).

* To whom correspondence should be addressed. Tel: +61(02)-6125-5894. Fax: +61(02)6125-5086. E-mail: Warwick.Hillier@anu.edu.au.

‡ The Australian National University.

§ Service de Bioénergétique, DBJC.

|| Russian Academy of Sciences.

⊥ Princeton University.

[1] Abbreviations: CA, carbonic anhydrase; Chl, chlorophyll; EZ, ethoxyzolamide; MIMS, membrane inlet mass spectrometry; PSII, photosystem II; OEC, oxygen evolving site; VMSOW, Vienna mean standard ocean water.

[2] Chl *d* is the main pigment in the cyanobacterium *Acaryochloris marina* and is also found in some Rhodophytes. In these organisms, Chl *d* may comprise the photoactive pigment in the reaction center.

10.1021/bi051892o CCC: $33.50
Published on Web 01/27/2006

excitons to a specialized Chl *a* reaction center complex (historically termed P680), where charge separation occurs by reduction of a pheophytin *a* molecule. The electron hole left within the $P680^+$ complex is transferred to the OEC via the special redox-active tyrosine Y_Z and used in the substrate oxidation chemistry to produce O_2. Because the charge-separated state generated by the P680 complex is a one-electron event and the formation of O_2 is a four-electron event, sequential electron holes generated by the P680 complex in the light are stored in the $Mn_4O_XCa_1$ cluster until sufficient electron deficiency is reached to trigger the formation of molecular O_2. As such, the OEC cycles through a series of redox states, termed the S_n states (for $n = 0, 1, 2, 3, 4$), which are characterized by a unique periodicity of four in the O_2 yield produced by single-turnover light flashes (*10*, *11*). A broad range of hypothetical models have been proposed to account for the O_2-producing chemistry (*12*−*14*; for review, see ref *15*).

At present, there are six different classes of photosynthetic reaction centers that have been identified in the Earth's biosphere, based on the chemical nature of electron donors/acceptors and the oxidation potential of the photoactive pigments (*16*, *17*). Interestingly, from a structural viewpoint, the various types of reaction centers are not very different; yet, only the PSII reaction center is capable of meeting the thermodynamic demands for the oxidation of water into molecular O_2. The question thus arises as to how PSII first evolved.

In one hypothesis, it has been proposed that during the Archean geologic period, when atmospheric levels of CO_2 were 10^3-10^4 times higher than they are today and the O_2 content was considerably less, hydrated CO_2 in the form of bicarbonate (HCO_3^-) served as the substrate for O_2 formation in an ancestral, precursor PSII reaction center (*18*). Direct evidence from contemporary photoautotrophs to support this hypothesis is minimal, but arguments have been made as follows: (i) the free energy change for the oxidation of bicarbonate to O_2 vs water oxidation is expected to be more favorable (*18*); (ii) the $Mn(II)-HCO_3^-$ complexes that would have occurred naturally under the conditions predicted for the Archean oceans are likely to be efficient electron donors to the low potential forms of the ancestral reaction centers (*19*); (iii) in contemporary PSII physiology, bicarbonate greatly accelerates the photoassembly of the $Mn_4O_XCa_1$ cluster (*20*) while a "bicarbonate effect" is observed on the electron transfer on the oxidizing side of the P680 complex (*21*).

The bicarbonate effects in PSII have an extensive history (*22*−*24*), and a specific bicarbonate effect involving the PSII acceptor side electron transfer reaction between the two quinone electron carriers, Q_A and Q_B, is well-established (*25*, *26*). Indeed, it was found that bicarbonate binds directly to the nonheme Fe cofactor that is located between the two quinones (*26*). Interestingly, the acceptor-side bicarbonate effect has never been demonstrated to regulate electron flow in vivo.

The donor side bicarbonate effect has broader importance for an evolutionary role as a source of oxidizable substrate. Historically, there has been a long discussion as to the exact nature of the substrate for the O_2 produced by PSII. The pioneering experiments by Ruben, Randle, Kamen, and Hyde in 1941 (*27*) clearly shaped the early assignment of water as the substrate. These researchers found that the O_2 produced by cultures of green algae could be enriched in ^{18}O only when ^{18}O-labeled water was added to the medium and not when ^{18}O-labeled bicarbonate was added (*28*). However, these results could be questioned because the intrinsic carbonic anhydrase (CA) activity of the algae samples is expected to rapidly redistribute the oxygen isotopes between the bicarbonate and the solvent water, particularly at the low isotope enrichments and the long times (several minutes) used in these measurements (for a historical survey, see ref *24*).

Upon the discovery of the "bicarbonate effect" on PSII electron transfer, Warburg and Krippahl vigorously argued that a special "activated CO_2 complex" was the true substrate for O_2 (*29*, *30*). However, the early mass spectrometric studies under a variety of conditions always revealed that the isotopic composition of the O_2 produced mirrors the isotopic composition of the water (*27*, *28*, *31*, *32*). Despite this, Metzner and co-workers claimed evidence that photosynthetically generated O_2 can be transiently enriched in ^{18}O when ^{18}O-labeled bicarbonate is added (*33*). Because this transient ^{18}O enrichment seemed to disappear on a time scale slower than the rate of isotopic equilibration with the solvent water, Metzner hypothesized (*33*) that bicarbonate acts as a "shuttle" between the solvent water and the catalytic site. Thus, in this case, bicarbonate is the immediate precursor to O_2 while water is the ultimate source. Crucial to this proposal would be the necessary involvement of a PSII-associated CA, to rapidly rehydrate catalytic amounts of CO_2 that could easily be lost from the sample. Interestingly, evidence for a PSII-associated CA has been reported (*34*−*36*); yet, a bicarbonate intermediate that competes with water as the electron donor to PSII has never been identified.

Subsequent mass spectrometric measurements have contradicted, yet never totally invalidated, the transient isotope effect (*33*). The most direct indication of this effect were the experiments performed with ^{18}O-labeled bicarbonate that showed only a very small amount (<1%) of photogenerated ^{18}O-labeled O_2 and, hence, indicated a limited photooxidation of bicarbonate by PSII (*37*, *38*). Conclusive proof for this reaction was lacking due to CA-catalyzed isotopic redistribution. Other mass spectrometric measurements of isotopic fractionation (*39*, *40*) and water−ligand exchange (*9*, *41*−*44*) similarly do not preclude bicarbonate oxidation due to the intrinsic CA activity. In the most recent report on this question, optical measurements and mass spectrometry showed neither inhibition of S-state turnover under conditions of elevated CO_2 partial pressures, nor the appearance of $C^{18}O_2$ following $H_2{}^{18}O$ addition (*45*). These results excluded the release of labile CO_2 from PSII and subsequent rapid rehydration to bicarbonate. However, the nature of the experiments and the limited *s*/*n* of the measurements, like earlier work, still do not exclude limited bicarbonate oxidation in PSII and provides only a relative measure of CA activity (given as ^{18}O enrichment rate). Collectively, the body of experimental data thus far indicates that bicarbonate is unlikely to represent the principle physiological substrate for oxidation; yet, the question remains to what level of bicarbonate oxidation flux is possible, if any. Experiments that undertake quantification are needed, and central to this understanding is the intrinsic CA activity in PSII samples.

In this communication, we report our work to determine whether bicarbonate can act as a substrate for O_2 production, either as part of the basic mechanism or in terms of a "genetic memory" of some ancestral chemistry for bicarbonate oxidation (*18*). Over the last several years, we have been exploiting the use of special time-resolved (millisecond range) mass spectrometric techniques developed in our lab (*9*, *42*−*44*) to follow the rate of ^{18}O incorporation into the O_2 produced by PSII from ^{18}O-labeled water. Here, we extend these measurements to quantitatively determine any possible ^{18}O flux from ^{18}O-labeled bicarbonate into the O_2 produced. We have used a broad range of PSII-enriched preparations and have placed a particular emphasis on calculating the effects of the intrinsic CA activity of the samples to know the exact bicarbonate concentration at the time of the measurement. The results clearly show that water is the physiologically significant substrate for photosynthetic O_2 production, yet do identify a small flux from labeled bicarbonate. Results from this work were first presented at the 13th International Photosynthesis Congress Proceeding (*46*).

MATERIALS AND METHODS

Spinach PSII-Enriched Membrane Fragments. The spinach fragments were prepared from fresh thylakoids using 5% Triton X-100 detergent (*47*) and stored as small beads at −80 °C until use.

Thermosynechococcus elongatus PSII Core Complexes. The PSII core complexes were prepared using the detergent solubilization and ion exchange purification (metal binding−polyhistidine binding) methods described earlier (*48*).

Arthrospira maxima PSII Thylakoids. The PSII thylakoids were prepared from log phase cells harvested by filtration. Cells were washed with a medium consisting of 100 mM HEPES at pH 7.5, 15 mM $MgCl_2$, and 15 mM $CaCl_2$ before a second wash in the same medium supplemented with 1.2 M betaine and 10% glycerol. The cells were disrupted by a French pressure cell, and cell debris was separated by a 3000*g* centrifugation for 10 min. The supernatant was then centrifuged for 30 min at 200000*g* to collect the thylakoid membranes, which were resuspended in a small volume of the second wash medium.

Oxygen Activity. Steady state rates of O_2 evolution for spinach, *T. elongatus*, and *A. maxima* were ∼600, ∼3000, and ∼220 μmol O_2 (mg of Chl)$^{-1}$ h^{-1}, respectively, in the presence of 500 μM *p*-phenyl benzoquinone and 500 μM $K_3Fe(CN)_6$.

Labeled Bicarbonate. Stock solutions were prepared by incubating 800 mM $NaHCO_3$ in ^{16}O-enriched (at natural abundance) or ^{18}O-enriched (96% atom ^{18}O enrichment, Isotec) solvent water for >24 h to achieve complete isotopic equilibration. Individual bicarbonate injections were prepared by freeze drying aliquots of the 800 mM bicarbonate stock solutions. The solid bicarbonate aliquots were then redissolved in degassed $H_2{}^{16}O$ (natural abundance) resulting in stock solutions containing bicarbonate enriched at >96% or natural abundance (0.2%) levels of ^{18}O. All stocks were prepared and used immediately after resuspension (handling time ∼15 s), minimizing isotopic exchange of ^{18}O label in $HC^{18}O_3$ back into the solvent water. Aliquots of the stock bicarbonate solutions were added to the sample chamber to give a final bicarbonate concentration of 50 mM. To assay the uncatalyzed and CA-catalyzed rates of isotopic exchange between ^{18}O-labeled bicarbonate and the solvent water, $^{13}C/^{18}O$-labeled bicarbonate was used (i.e., $H^{13}C^{18}O_3^-$) to separate out the background $^{12}CO_2$ signals. We note that removing the solvent by either evaporation or vacuum stripping while in the liquid phase could result in the total loss of ^{18}O via exchange. However, we found that the freeze-dried bicarbonate stocks retained >98% ^{18}O recoverable in the solid.

Mass Spectrometric Measurements. MS measurements were performed at Chl concentrations of 0.5, 0.1, and 0.3 mg/mL for the spinach, *T. elongatus*, and *A. maxima* samples, respectively. Measurements were made at 10.0 °C in a medium consisting of 100 mM HEPES at pH 7.5, 1.2 M betaine, 10% glycerol, 15 mM $MgCl_2$, 15 mM $CaCl_2$ in the presence of 0.1 mM *p*-phenyl benzoquinone, and 0.5 mM $K_3Fe(CN)_6$ as the electron acceptors and 10 μM ethoxyzolamide (EZ) as a CA inhibitor. In certain experiments, 3 units of CA (bovine erythrocytes, Fluka) were added in the absence of EZ to accelerate $HCO_3^- \leftrightarrow CO_2$ interconversion. Isotopic determination of the O_2 produced by the sample was measured simultaneously at $m/e = 32$, 34, and 36 ($^{16,16}O_2$, $^{16,18}O_2$, and $^{18,18}O_2$, respectively) and $m/e = 45$, 47, and 49 for ^{13}C-labeled carbon dioxide ($^{13}C^{16,16}O_2$, $^{13}C^{16,18}O_2$, and $^{13}C^{18,18}O_2$, respectively). Measurements were made using a membrane inlet mass spectrometer (MIMS) consisting of a custom-built sample chamber interfaced to a Micromass Isoprime mass spectrometer (GV Instruments). The O_2 signals were determined from the peak heights as described earlier (*42*, *43*). Atmospheric CO_2 was not removed from the sample or the suspension medium. Samples were illuminated by 16 saturating light flashes (5 Hz repetition rate) generated by a xenon flash lamp (EG&G).

Data Analysis and Fitting. Least squares data fitting was performed with Excel (Microsoft) using the inbuilt solver function for optimizing nonlinear problems according to the generalized reduced gradient (GRG2) algorithm. The variables k_1, k_2, and k_{leak} were solved by minimization of the residuals from a model described in the text. Additional parameters required to reach the solution were as follows: (i) the added bicarbonate concentration, (ii) the ^{18}O enrichment of the bicarbonate (fixed at 96%), and (iii) a kinetic parameter ($k_{transport}$) to compensate for the diffusion of the CO_2 across the membrane (important for times $t < 15$ s). The initial C_0, C_1, and C_2 concentration terms were set to zero and the initial B_0, B_1, B_2, and B_3 were determined by added bicarbonate concentration and ^{18}O enrichment. The errors in the parameters were obtained from the macro (*49*) that calculates the diagonal elements of the error matrix (*50*, *51*). The error matrix is defined as the inverse of the curvature matrix **M** where $m_{ij} = \Sigma\, \partial F/\partial a_i\, \partial F/\partial a_j$ and $y_{fit} = F(x; a_i, a_j, ...)$. Uncertainty in the predicted ^{18}O concentrations (from $HC^{18}O_3^- \rightarrow H_2{}^{18}O$ leakage) was based on calculated errors in the fitted parameters. The ^{18}O leakage contribution was first calculated from fit parameters, and the uncertainty in this value was derived from the maximum deviation obtained using $k_1 \pm 1$ SD and $k_2 \pm 1$ SD. This is further outlined in the Supporting Information (S1). The ^{18}O concentration was insensitive to the other fitting parameters in the model.

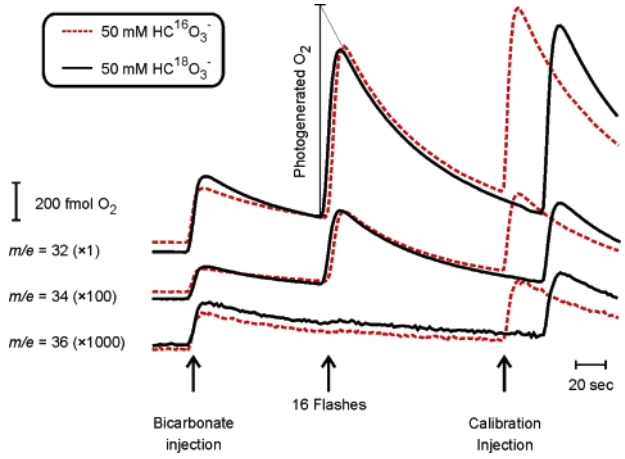

FIGURE 1: Oxygen traces of $^{16,16}O_2$, $^{16,18}O_2$, and $^{18,18}O_2$ in the presence of 50 mM $HC^{18}O_3^-$ at greater than 96% ^{18}O enrichment (solid line) and with 50 mM HCO_3^- at natural abundance (dashed line) for spinach PSII membrane fragments at 0.5 mg mL^{-1}. The first initial rise in the data coincides with bicarbonate injection and represents an O_2 background signal. The signal then stabilizes for 60 s delay before a 5 Hz flash train of 16 flashes liberates photosynthetic O_2. A third peak is the injection calibration of 5 μL of air-saturated water, pre-equilibrated at 25 °C. The detection level is >0.02 pmol and signals were determined from peak heights, i.e., consumption rate extrapolated to the beginning of the flash train.

RESULTS

For the purpose of this study, we examined three different types of samples: (i) PSII-enriched membranes from spinach (>95% PSII centers), which represents an extensively characterized higher plant material used in oxygenic studies; (ii) isolated PSII core complexes from *T. elongatus* (comprised of ca. 19 polypeptide subunits), from which the midresolution (3.5 Å) crystal structure has been obtained (*7*); and (iii) crude thylakoid membranes from *A. maxima*, which is a cyanobacterium that grows naturally in the high alkaline (bi)carbonate (>400 mM) environment of an African soda lake and has been recently characterized as having the highest OEC turnover efficiency of any cyanobacterium or higher plant (*52*). These three samples thus provide a broad survey of organisms to examine the role of bicarbonate as a possible substrate for O_2 production.

Figure 1 shows the mass spectrometric measurements of the light-induced O_2 produced by the three samples in the presence of ^{18}O-enriched and natural abundance 50 mM bicarbonate. The data at $m/e = 32$ and 34 (for $^{16,16}O_2$ and $^{18,16}O_2$, respectively) clearly show the photogenerated oxygen signals. The data at $m/e = 36$ (for $^{18,18}O_2$) were also recorded, but the signal amplitudes were too small (~0.04 pmol) to be able to detect reliably any differences in the $^{18,18}O_2$ produced in the presence of natural abundance and 96% ^{18}O-enriched 50 mM bicarbonate. Furthermore, calibration of the $m/e = 36$ signals is problematic because of the large ^{36}Ar background signal.[3] Therefore, the analysis of the MIMS measurements was restricted to the $m/e = 32$ and 34 data.

For a given ^{18}O enrichment (ϵ), the various molecular oxygen species follow a binomial distribution, i.e.,

$$(m/e)\ 32{:}34{:}36 = (1-\epsilon)^2{:}2\epsilon(1-\epsilon){:}\epsilon^2 \qquad (1)$$

where m/e 32 + 34 + 36 = 100%.

According to this relationship, any increase in the ^{18}O enrichment will give rise to an increase in the $^{16,18}O_2$ signal and a decrease in the $^{16,16}O_2$ signal. Because these O_2 signals can be accurately measured separately, the ratio of the $m/e = 34$ to $m/e = 32$ data provides a highly sensitive probe of the ^{18}O distribution in the photogenerated O_2 that, in turn, is indicative of the ^{18}O enrichment of the substrate. The experimental results for the three types of PSII samples are presented in Table 1, in which the measurements were made in the presence of either 50 mM bicarbonate at natural abundance or 50 mM bicarbonate enriched to 96% ^{18}O. The upper part of Table 1 shows the measured 34/32 mass ratios for the O_2 produced, while the lower part shows the calculated ^{18}O isotope enrichments of the substrate. In the presence of 50 mM bicarbonate enriched to 96% ^{18}O, there is a small (~5−8% relative) increase in the ^{18}O enrichment of the O_2 produced, as compared to the measurement in the presence of 50 mM bicarbonate at natural abundance for all three PSII samples.

To determine whether this small but significant increase in the ^{18}O enrichment is due to bicarbonate as a substrate or to isotopic exchange between the added bicarbonate and the solvent water, additional tests were made. The redistribution of the ^{18}O isotope between the bicarbonate and the solvent water results from the chemical interconversion between bicarbonate and dissolved CO_2, i.e.,

$$HCO_3^- + H^+ \leftrightarrow H_2CO_3 \underset{k_2}{\overset{k_1}{\rightleftharpoons}} CO_2 + H_2O \qquad (2)$$

The first step of this reaction is a rapid acid/base equilibrium followed by a rate-limiting reversible hydration (k_1)/dehydration (k_2) reaction (*53*) that is greatly accelerated by CA activity (*54*).

To determine the exact concentration of ^{18}O-labeled bicarbonate available to PSII at the time of the mass spectrometric measurement, we determined the extent and time dependence of the intrinsic CA activity for each PSII sample. This was achieved by adding $H^{13}C^{18}O_3^-$ to the samples and then following the time-dependent speciation of the CO_2 gas measured at $m/e = 49$, 47, and 45 (*55*, *56*) as shown in Figure 2 for spinach. The complex behavior in Figure 2 reveals an initial rapid rise at $m/e = 49$ that represents the chemical equilibration between aqueous $H^{13}C^{18}O_3^-$ and gaseous $^{13}C^{18}O_2$, which occurs in parallel with a slower isotopic equilibration process. The ^{18}O isotope equilibration between bicarbonate and water occurs via two routes in solution, the acid-catalyzed pathway in eq 2 (which is dominant at pH < 8) and a slower direct dissociation of hydroxide that becomes increasingly important at more alkaline pH (*55*). The ^{18}O isotope equilibration is measurable from the slower transient changes of the $^{13}C^{18,18}O_2$, $^{13}C^{16,18}O_2$, and $^{13}C^{16,16}O_2$ species at $m/e = 49$, 47, and 45, respectively. Ultimately, the solvent water provides the final sink for the ^{18}O redistribution and gradually undergoes an increase in ^{18}O enrichment with time above natural abundance.

The change in the ^{18}O enrichment with time can be given as the change in ^{18}O atom fraction (χ^{18}_O) with time. The ^{18}O atom fraction for carbon dioxide is given as:

[3] ^{36}Ar has a natural abundance of 0.34% and is ~20 times less soluble in water than O_2.

Table 1: Measured Oxygen $m/e = 34/32$ Ratios and Corresponding ^{18}O Enrichments (ϵ) for Photosynthetic Oxygen Evolution in the Presence of Labeled and Unlabeled Bicarbonate Measured at 60 s after Mixing in Three Different PSII-Containing Samples

	oxygen ratios (34/32) × 100		
sample	substrate as 50 mM $NaHC^{16}O_3$	substrate as 50 mM $NaHC^{18}O_3$	CA equilibrated 50 mM $NaHC^{18}O_3$
spinach[a]	0.382 ± 0.003	0.404 ± 0.003	0.911 ± 0.010
T. elongatus[b]	0.384 ± 0.005	0.407 ± 0.004	0.912 ± 0.010
A. maxima[c]	0.384 ± 0.003	0.416 ± 0.003	0.911 ± 0.017
	^{18}O enrichment (%)[d]		
spinach	0.191 ± 0.002	0.202 ± 0.002	0.453 ± 0.005
T. elongatus	0.192 ± 0.002	0.203 ± 0.002	0.454 ± 0.005
A. maxima	0.192 ± 0.002	0.208 ± 0.002	0.453 ± 0.005

±SE (n) = 7−8. Oxygen $m/e = 32$ signals following 16 flashes. [a] 1136 pmol. [b] 827 pmol. [c] 184 pmol. [d] ^{18}O enrichment is determined from eq 1.

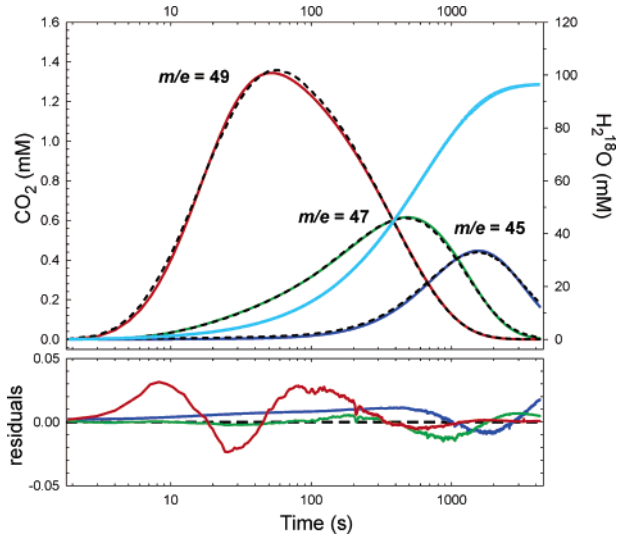

FIGURE 2: Profile of CO_2 species following injection of 50 mM $H^{13}C^{18}O_3^-$ into the cuvette containing 0.5 mg mL^{-1} spinach PSII membrane fragments and 10 μM EZ. For both the experimental data (dashed black lines) and the fitted data, $m/e = 49$ (red), $m/e = 47$ (green), and $m/e = 45$ (blue) are presented. A second ordinate axis depicts the ^{18}O concentration (mM) of water as the ^{18}O bicarbonate undergoes isotopic equilibration (cyan). The final ^{18}O enrichment of the water does not reach 150 mM due to the consumption parameter (k_{leak}) and the true final concentration of ^{18}O carries an additional contribution from natural abundance (~110 mM $H_2{}^{18}O$). A lower plot gives the residuals between the measured data and the fits (mM CO_2) for the following traces: $m/e = 49$ (red), $m/e = 47$ (green), and $m/e = 45$ (blue). The maximum residual occurs for the $m/e = 49$ data and represents 12% of the instantaneous CO_2 signal or ~±2% of maximum CO_2 signal.

$$\chi_{^{18}O} = \frac{(47) + 2(49)}{2[(45) + (47) + (49)]} \tag{3}$$

A plot of the natural log($\chi_{^{18}O}$) for CO_2 vs time is linear (*53*) and gives a negative first-order rate constant as the ^{18}O enrichment of CO_2 decreases, ultimately maximizing $m/e = 45$ CO_2 as the ^{18}O appears in the solvent water. Figure 3 depicts a plot of the ^{18}O enrichment vs time while the relative rates normalized to the uncatalyzed rate (i.e., in the absence of the sample) are given in Table 2. The results indicate that the rate of loss of ^{18}O from $^{13}C/^{18}O$-labeled bicarbonate, or the rate of CA activity, varies among the different PSII samples when compared to the uncatalyzed rate (*34*−*36*), despite the presence or absence of 10 μM EZ, which is a standard inhibitor of CA activity. Notably, there is a considerably higher CA activity in the spinach PSII-enriched sample as compared to the two cyanobacterial samples, which are a highly purified PSII core complex from *T. elongatus* and a crude thylakoid preparation from *A. maxima*. A comparison of the intrinsic CA rates with and without the EZ inhibitor revealed that the CA rates of the two cyanobacterial samples are relatively low (1.5−1.9 × uncatalyzed rate) and independent of the inhibitor while the spinach sample has a much larger intrinsic CA rate (35 × uncatalyzed rate) (Figure 3) than when the inhibitor EZ is present (5.7 × uncatalyzed rate) (Table 2). Higher concentrations of the EZ inhibitor were not used because of interference with the normal PSII reactions.

To determine the empirical time-dependent increase in ^{18}O enrichment of the solvent water from the measured rate of loss of the ^{18}O enrichment of the bicarbonate, a kinetic analysis is required. Using the experimental data measured at $m/e = 49$, 47, and 45, a set of differential equations were developed to fit the time-dependent changes in [CO_2]. These equations incorporate the rate constants k_1 (hydration) and k_2 (dehydration) in eq 2, along with an additional rate constant k_{leak}, which reflects the rate of CO_2 loss across the MIMS membrane under vacuum. The series of differential equations is given below, where C_0, C_1, and C_2 are the unlabeled, single, and double ^{18}O-labeled CO_2 and B_0, B_1, B_2, and B_3 are the unlabeled, single, double, and triple ^{18}O-labeled HCO_3^-.

$$\frac{d[C_0]}{dt} = k_2\left(B_0 + \frac{1}{3}B_1\right) - k_1(C_0) - k_{leak}(C_0)$$

$$\frac{d[C_1]}{dt} = k_2\frac{2}{3}(B_1 + B_2) - k_1(C_1) - k_{leak}(C_1)$$

$$\frac{d[C_2]}{dt} = k_2\left(\frac{1}{3}B_2 + B_3\right) - k_1(C_2) - k_{leak}(C_2)$$

$$\frac{d[B_0]}{dt} = k_1(C_0) - k_2(B_0)$$

$$\frac{d[B_1]}{dt} = k_1(C_1) - k_2(B_1)$$

$$\frac{d[B_2]}{dt} = k_1(C_2) - k_2(B_2)$$

$$\frac{d[B_3]}{dt} = -k_2(B_3) \tag{4}$$

This type of analysis has been discussed earlier (*57*, *58*), but its use here represents the first application to solving the [CO_2] time-dependent MIMS data. The calculated values of the rate constants k_1, k_2, and k_{leak} obtained from the experimental fits for each PSII sample along with the uncatalyzed reactions are given in Table 2. The k_1 and k_2 rates for the uncatalyzed reaction are in close agreement with earlier determinations (*59*, *60*). The k_{leak} rate representing membrane consumption is relatively high due to the highly

Table 2: Rate of Isotopic Enrichment and Rate Constants for the $CO_2 \leftrightarrow HCO_3^-$ Equilibria with Various PSII Samples and the Calculated ^{18}O Leakage into Water 60 s after Injection of 50 mM Labeled Bicarbonate

sample	relative rates of CA activity[b]	calculated rate constants (s^{-1})[c]			calculated ^{18}O at 60 s[d]	
		k_1 ($\times 100$)	k_2 ($\times 100$)	k_{leak} ($\times 100$)	$[H_2{}^{18}O]$ (mM)[a]	$[H_2{}^{18}O]$ ϵ (%)
spinach	$\times 5.7$	8.92 ± 0.08	0.355 ± 0.003	1.63 ± 0.01	9.62 ± 0.08	0.0173 ± 0.0002
T. elongatus	$\times 1.5$	2.73 ± 0.03	0.109 ± 0.001	1.61 ± 0.02	3.06 ± 0.03	0.0054 ± 0.0001
A. maxima	$\times 1.9$	3.37 ± 0.05	0.134 ± 0.002	1.40 ± 0.02	3.74 ± 0.05	0.0067 ± 0.0001
uncatalyzed[a]	$\times 1$	1.92 ± 0.04	0.076 ± 0.002	1.27 ± 0.03	2.15 ± 0.06	0.0039 ± 0.0001

[a] Uncatalyzed rate in assay medium. [b] Value determined from eq 3 and normalized to the uncatalyzed rate in the assay medium. [c] Value determined from eq 4 after least-squares fitting. [d] Values determined from eq 5 do not include natural abundance.

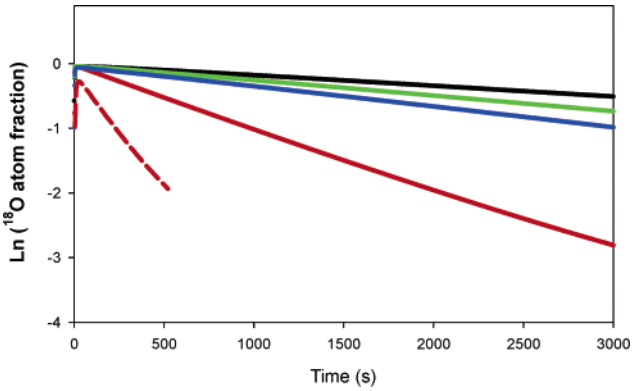

FIGURE 3: Change in the ^{18}O atom fraction ($\chi_{^{18}O}$) of CO_2 with time for the different PSII samples is shown as a measure of the intrinsic CA activity of a sample. All traces with solid lines were recorded in the presence of 10 μM EZ and the dashed line without. Relative CA rates as compared to the uncatalyzed reaction were as follows: Spinach, $\times 5.7$ (red line); spinach (uninhibited), $\times 35$ (dashed red line); *T. elongatus*, $\times 1.5$ (green line); *A. maxima*, $\times 1.9$ (blue line); and the uncatalyzed rate, $\times 1$ (black line). Only the spinach PSII membrane exhibits a substantial intrinsic CA activity, and this activity was suppressed in part by EZ.

permeable silicone membrane[4] used in this work. The accuracy of the fits to the model is shown in Figure 2 as the colored lines as compared to the dashed experimental data. The kinetic fit parameters show high statistical correlation coefficients, small residuals (as shown, for example, in the lower part of Figure 2), and small errors in the kinetic parameters (as shown in Table 2). Taken together, these features indicate the overall success of this model in describing the kinetic processes.

The fitted k_2 rate for the dehydration reaction was then used to empirically quantify the rate of increase in the ^{18}O concentration in the solvent water due to the isotope equilibration with the ^{18}O-labeled bicarbonate according to the following equation:

$$\frac{d[H_2{}^{18}O]}{dt} = k_2\left(\frac{1}{3}B_1 + \frac{2}{3}B_2 + B_3\right) \quad (5)$$

The increase in the ^{18}O concentration of the solvent water was determined at 60 s, which is the time interval between the bicarbonate injection and the 16 flashes (at 5 Hz) used to generate O_2. The ^{18}O concentration increases for the three PSII samples, and for the uncatalyzed reaction, they are given in Table 2. For the uncatalyzed reaction, the ^{18}O concentration increase is $\sim$2 mM, and for the spinach sample, which has the largest CA activity, it is $\sim$10 mM. Table 2 also presents the ^{18}O concentration increases in terms of ^{18}O enrichment (ϵ). These ^{18}O enrichments represent the incremental enrichments over natural abundance. The ^{18}O enrichments from Table 2, when added to the background enrichments at natural abundance in the presence of 50 mM $HC^{16}O_3^-$ in Table 1, define the effective overall background ^{18}O enrichments of the samples and are 0.208, 0.197, and 0.199% for spinach, *T. elongatus*, and A. *maxima*, respectively. These results should then be compared to the measured ^{18}O enrichments in the presence of 50 mM $HC^{18}O_3^-$ as shown in Table 1. These ^{18}O enrichment values are 0.202, 0.203, and 0.208% for spinach, *T. elongatus*, and *A. maxima*, respectively. A difference between the two data sets thus indicates an additional net ^{18}O flux into the photosynthetically produced O_2.

As a control experiment, samples containing the 50 mM bicarbonate enriched to 96% ^{18}O were incubated in the presence of 3 units of exogenously added CA (in the absence of the EZ inhibitor) to completely equilibrate the ^{18}O between the bicarbonate and the solvent water. Under this condition, a large 2.6-fold increase in the ^{18}O enrichment of the solvent water occurs (Table 1). For all samples, the measured enrichment was $\sim$0.453%, which is highly consistent with the predicted enrichment of 0.459%[5] arising from 50 mM bicarbonate (enriched at 96% ^{18}O) that is fully isotope equilibrated with the solvent water.

DISCUSSION

Photosynthetic Oxygen Signals. In earlier studies we probed the kinetic isotope exchange of the substrate at the OEC using ^{18}O-labeled water as a function of the oxidation states (*9*). This work revealed that there are two dissimilar ^{18}O exchange rates in PSII samples from spinach, differing by ca. $20-10^4$ depending on the OEC oxidation state (no added bicarbonate and at atmospheric CO_2). The results indicated that the two substrate molecules bind at different sites throughout the S state cycle. However, these results do not reveal the chemical identity of the O donors, i.e., water vs rapidly exchanging bicarbonate. Given the rate constants of substrate exchange from our earlier work (*9*) and the initial 60 s delay between the bicarbonate injection and the 5 Hz flash train in the current work, all of the substrate sites will be fully equilibrated with labeled substrate at the time of measurement (accessibility issues between bicarbonate vs water aside). Accordingly, we can expect a distribution of ^{16}O- and ^{18}O-labeled product O_2 according to eq 1 if

[4] The k_{leak} rate of CO_2 consumption in Table 2 shows variation due to differential membrane fouling.

[5] The oxygen percentage enrichment is $[HCO_3^-]/[H_2O]$; i.e., $[(0.96 \times 0.05 \times 3)/55.55] \times 100$, which is additive to a natural abundance level of 0.2%.

bicarbonate binds at both substrate-binding sites. If, on the other hand, bicarbonate binds only at one substrate-binding site, then the ^{18}O enrichments of the O_2 products measured at $m/e = 32$ and 34 will be determined by the ^{18}O enrichment (ϵ) of bicarbonate alone: i.e., $32:34:36 = 1 - \epsilon:\epsilon:0$. From this, it can be seen that the double-labeled $m/e = 36$ product will not be produced at all; however, because of the low ^{18}O levels of the solvent water, the $m/e = 36$ signal in these experiments (see Figure 1) is extremely small making mechanistic interpretations based on this signal difficult. Therefore, in our analysis, we have concentrated on the 34/32 mass ratio to provide a measure of bicarbonate oxidation that involves binding to only one of the two substrate-binding sites. The isotope ratio experiment as we present here, however, greatly improves the accuracy of the measurements.

The 34/32 mass ratio for each sample measured with natural abundance bicarbonate should yield an ^{18}O enrichment value from eq 1 that represents natural abundance levels, i.e., 0.204% (*61*). The photosynthetically generated signals fell reproducibly and consistently below this enrichment level even in the absence of any added bicarbonate (data not shown). The reason for this discrepancy was not calibration or a lower ^{18}O enrichment of Canberra water (typically −6‰ vs VSMOW; i.e., a final $\epsilon = 0.199\%$) or the equilibrium isotope effects in bicarbonate. The explanation for this phenomenon is due to a process of isotopic fractionation arising from diffusion of the O_2 products in the membrane inlet system used for sampling the cuvette. Diffusion according to mass favors the lighter isotope (Graham's law of effusion), and this will isotopically change the 34/32 ratio and the ^{18}O enrichment to a value that is similar to that reported in Table 1, i.e., rate (34)/rate (32) = $\sqrt{32}/\sqrt{34} = 0.97 \times 0.199\%$.

Bicarbonate as a Substrate. In the present study, bicarbonate concentrations were maximized by conducting the measurements at pH 7.5, where the bicarbonate p*K* equilibria strongly favors the HCO_3^- anion (~95%). At pH 7.5, the existing [HCO_3^-] in solution from atmospheric sources (350 ppm CO_2, 950 mBar, 10 °C) is ~210 μM. The added ^{18}O-labeled bicarbonate concentration in our measurements is ~47.5 mM, which is 200-fold greater than the residual [HCO_3^-] in solution and represents a 480-fold increase in the ^{18}O enrichment over natural abundance. Thus, the added bicarbonate swamps out any effects of the naturally occurring ^{18}O species. In comparison with the conditions of the earlier measurements that have favored either water (*27*, *28*, *31*, *32*, *38*, 39) or bicarbonate (*33*, *62*), our measurements were carried out with bicarbonate at both high concentrations (50 mM) and high enrichments (>96%) as well as with PSII samples that were free of any additional side reactions involving O_2 uptake processes. Thus, our measurements should provide the most definitive answer as to whether there is any oxygen flux from bicarbonate to molecular O_2.

To test the possibility that bicarbonate can serve as a substrate for O_2 production by PSII, we determined the precise ^{18}O isotopic distribution between the O_2 produced, the pool of labeled bicarbonate, and the solvent water. The intrinsic CA activities of the PSII preparations, which facilitate isotope equilibration between the bicarbonate and the solvent water, were initially suppressed by the addition of the inhibitor EZ. As revealed in Table 1, there are small, but significant, differences between the ^{18}O enrichment of the O_2 produced in the presence of 50 mM bicarbonate at natural abundance and in the presence of 50 mM bicarbonate containing 96% ^{18}O. The measured ^{18}O enrichment differences are 0.011 ± 0.003% for spinach, 0.011 ± 0.003% for *T. elongatus*, and 0.016 ± 0.003% for *A. maxima*. However, because the inhibitor EZ did not completely suppress all of the CA activity, the residual CA activity of each sample was kinetically modeled and the rate constant for the isotopic equilibrium reaction was derived (Table 2), which was used to empirically predict the increase in ^{18}O enrichment of the water (and hence of the O_2 product) above natural abundance (Table 2). The enrichment was determined. The ^{18}O leakage due to the residual CA activities was calculated to be the following: 0.017% for spinach, 0.005% for *T. elongatus*, and 0.007% for *A. maxima*. The error estimates in determining the rate constants by eq 5 were extremely small (±0.0001) relative to the experimental signals and thus can be disregarded.

Upon correction for the ^{18}O leakage due to the residual CA activity over the time of the measurement, the calculated net ^{18}O flux to the O_2 produced by each sample is as follows: −0.006 ± 0.003% for spinach, 0.006 ± 0.003% for *T. elongatus*, and 0.009 ± 0.003% for *A. maxima*. The calculated net value for spinach is negative and is outside of the error limit. The reason for this negative value is unknown at present but is most likely due to the inability of the EZ inhibitor to fully suppress the substantially higher intrinsic CA activity of the spinach sample, resulting in a slight overestimation of the ^{18}O leakage rate. Figure 3 illustrates directly the large intrinsic CA activity of PSII membrane fragments and the level suppressed by EZ. In spinach thylakoids, this level is even greater (results not shown). In contrast, the net calculated values for the two cyanobacteria samples are positive and are also outside the limits of error. In this case, the source of the additional ^{18}O enrichments might be due to an underestimation of the intrinsic CA activity. However, if this were true, then the dehydration rate constant k_2 would be considerably different, well outside of the error limit in the analysis. For example, to accommodate the entire ^{18}O enrichment in the O_2 product arising from labeled bicarbonate exchange with water in the *A. maxima* samples (i.e., an overall difference of 0.016% enrichment in Table 1), the intrinsic CA rate would have to be faster by a factor of ~3. Such a rate is closer to what is seen in spinach than in the cyanobacteria. Thus, quite interestingly, our analysis of *A. maxima*, an obligate bicarbonate-requiring prokaryote, and to a lesser degree of *T. elongatus*, reveals an unaccounted ^{18}O flux that is outside of the experimental error and may very well originate from bicarbonate oxidation.

A general analysis of the enrichment behavior can be seen in Figure 4 which shows the relationship between the measured $m/e = 34/32$ ratio, the ^{18}O enrichment of the sample, and the occupancy of the catalytic site. If bicarbonate oxidation takes place in the OEC of PSII, then the addition of 50 mM-labeled bicarbonate should be sufficient to saturate a substrate-binding site with a physiologically relevant K_M. In such a case, there would be a dramatic increase in the $m/e = 34/32$ ratio. The K_M for bicarbonate stimulation of the O_2 evolution at an interaction site on the donor side of PSII has been estimated to be about 10−20 μM (*22*),

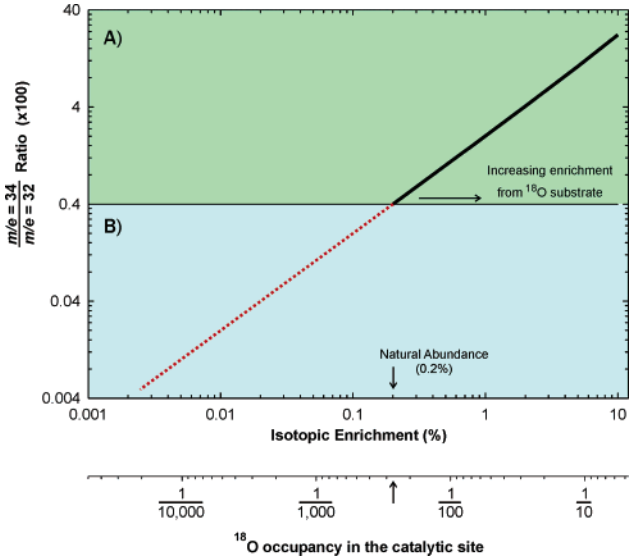

FIGURE 4: Oxygen $m/e = 34/32$ ratios derived from both levels of ^{18}O enrichment and on the second abscissa the ^{18}O occupancy in the catalytic site. The upper figure (A) presents the increasing $m/e = 34/32$ oxygen ratio in relation to the ^{18}O enrichment and correlates with the data presented in Table 1. The lower figure (B) presents a means for accessing the small differences between experiments and estimating the ^{18}O occupancy in the catalytic site.

although the rate of stimulation is modest as compared with the bicarbonate effect on the acceptor side (*25*). If the donor side interaction site is reflecting a substrate site, then the added 50 mM ^{18}O-labeled bicarbonate should have saturated the binding site and the corresponding 34/32 ratio would have increased dramatically. For example, if there is a hypothetical 10% occupancy of one substrate site with labeled bicarbonate, the expected 34/32 ratio would be 12, i.e., a 30-fold increase over the natural abundance levels of water. The net positive changes in ^{18}O enrichment values observed in this study for the cyanobacteria samples are exceedingly small (i.e., 0.006−0.010% or a 3.6−5.2% differential increase over unlabeled bicarbonate) and indicate that the site with a K_M of 10 μM cannot be a substrate site. The analysis in Figure 4 reveals that the small net increases in the ^{18}O enrichment observed would represent bicarbonate occupancy in less than 1 per 5000 reaction centers. Such results indicate that bicarbonate cannot be a physiologically significant substrate in contemporary PSII and that by far the bulk of the oxygen flux comes from water. The exceedingly low levels of bicarbonate oxidation may arise as a side reaction in altered or damaged PSII reaction centers or may reflect the ancestral chemistry that used bicarbonate as a transitional electron donor to PSII (18).

NOTE ADDED IN PROOF

The recent 3.0 Å PSII structure (*63*) provides no further bicarbonate interactions in PSII other than the bicarbonate/non-heme iron association of the acceptor side.

ACKNOWLEDGMENT

We thank Michael Bender (Princeton) for fruitful discussions and Joseph Billo (Boston College) and Jeff Wood (ANU) for statistical consultation.

SUPPORTING INFORMATION AVAILABLE

Further description of the error values obtained for the calculated ^{18}O after 60 s based on the fitted k_1 and k_2 rates. This material is available free of charge via the Internet at http://pubs.acs.org.

REFERENCES

1. Summons, R., Jahnke, L., Hope, J., and Logan, G. (1999) 2-Methylhopanoids as biomarkers for cyanobacterial oxygenic photosynthesis, *Nature 400*, 554−557.
2. Rye, R., and Holland, H. D. (1998) Paleosols and the evolution of atmospheric oxygen: A critical review, *Am. J. Sci. 298*, 621−672.
3. Kasting, J. F. (2001) Earth history−The rise of atmospheric oxygen, *Science 293*, 819−820.
4. Blankenship, R. E., and Hartman, H. (1998) The origin and evolution of oxygenic photosynthesis, *Trends Biochem. Sci. 23*, 94−97.
5. Olson, J. M., and Blankenship, R. E. (2004) Thinking about the evolution of photosynthesis, *Photosynth. Res. 80*, 373−386.
6. Kamiya, N., and Shen, J.-R. (2003) Crystal structure of oxygen-evolving photosystem II from *Thermosynechococcus vulcanus* at 3.7-Å resolution, *Proc. Natl. Acad. Sci. U.S.A. 100*, 98−103.
7. Ferreira, K. N., Iverson, T., Maghlaoui, K., Barber, J., and Iwata, S. (2004) Architecture of the photosynthetic oxygen-evolving center, *Science 303*, 1831−1838.
8. Biesiadka, J., Loll, B., Kern, J., Irrgang, K. D., and Zouni, A. (2004) Crystal structure of cyanobacterial photosystem II at 3.2 angstrom resolution: A closer look at the Mn-cluster, *Phys. Chem. Chem. Phys. 6*, 4733−4736.
9. Hillier, W., and Wydrzynski, T. (2004) Substrate water interactions within the Photosystem II oxygen evolving complex, *Phys. Chem. Chem. Phys. 6*, 4882−4889.
10. Joliot, P., Barbieri, G., and Chabaud, R. (1969) Un nouveau modele des centres photochimiques du systeme II, *Photochem. Photobiol. 10*, 309−329.
11. Kok, B., Forbush, B., and McGloin, M. (1970) Cooperation of charges in photosynthetic oxygen evolution. I. A linear four step mechanism, *Photochem. Photobiol. 11*, 457−475.
12. McEvoy, J. P., and Brudvig, G. W. (2004) Structure-based mechanism of photosynthetic water oxidation, *Phys. Chem. Chem. Phys. 6*, 4754−4763.
13. Dasgupta, J., van Willigen, R. T., and Dismukes, G. C. (2004) Consequences of structural and biophysical studies for the molecular mechanism of photosynthetic oxygen evolution: Functional roles for calcium and bicarbonate, *Phys. Chem. Chem. Phys. 6*, 4793−4802.
14. Lundberg, M., and Siegbahn, P. E. M. (2004) Theoretical investigations of structure and mechanism of the oxygen-evolving complex in PSII, *Phys. Chem. Chem. Phys. 6*, 4772−4780.
15. Hillier, W., and Messinger, J. (2005) Mechanism of photosynthetic oxygen production, in *Photosystem II: The Water: Plastoquinone Oxidoreductase in Photosynthesis* (Wydrzynski, T., and Satoh, K., Eds.) pp 567−608, Springer, The Netherlands.
16. Blankenship, R. E. (1992) Origin and early evolution of photosynthesis, *Photosynth. Res. 33*, 91−111.
17. Hillier, W., and Babcock, G. T. (2001) Photosynthetic reaction centers, *Plant Physiol. 125*, 33−37.
18. Dismukes, G. C., Klimov, V. V., Baranov, S. V., Kozlov, Y. N., DasGupta, J., and Tyryshkin, A. (2001) The origin of atmospheric oxygen on Earth: The innovation of oxygenic photosynthesis, *Proc. Natl. Acad. Sci. U.S.A. 98*, 2170−2175.
19. Kozlov, Y. N., Zharmukhamedov, S. K., Tikhonov, K. G., Dasgupta, J., Kazakova, A. A., Dismukes, G. C., and Klimov, V. V. (2004) Oxidation potentials and electron donation to photosystem II of manganese complexes containing bicarbonate and carboxylate ligands, *Phys. Chem. Chem. Phys. 6*, 4905−4911.
20. Baranov, S. V., Tyryshkin, A. M., Katz, D., Dismukes, G. C., Ananyev, G. M., and Klimov, V. V. (2004) Bicarbonate is a native cofactor for assembly of the manganese cluster of the photosynthetic water oxidizing complex. Kinetics of reconstitution of O_2 evolution by photoactivation, *Biochemistry 43*, 2070−2079.
21. Allakhverdiev, S. I., Yruela, I., Picorel, R., and Klimov, V. V. (1997) Bicarbonate is an essential constituent of the water-oxidizing complex of photosystem II. *Proc. Natl. Acad. Sci. U.S.A. 94*, 5050−5054.

22. Klimov, V. V., and Baranov, S. V. (2001) Bicarbonate requirement for the water-oxidizing complex of photosystem II, *Biochim. Biophys. Acta 1503*, 187−196.
23. Stemler, A., and Govindje. (1973) Bicarbonate ion as a critical factor in photosynthetic oxygen evolution, *Plant Physiol. 52*, 119−123.
24. Stemler, A. J. (2002) The bicarbonate effect, oxygen evolution, and the shadow of Otto Warburg, *Photosynth. Res. 73*, 177−183.
25. Wydrzynski, T., and Govindjee (1975) New site of bicarbonate effect in photosystem-II of photosynthesis—Evidence from chlorophyll fluorescence transients in spinach-chloroplasts, *Biochim. Biophys. Acta 387*, 403−408.
26. van Rensen, J. J. S., Xu, C., and Govindjee (1999) Role of bicarbonate in photosystem II, the water-plastoquinone oxidoreductase of plant photosynthesis, *Physiol. Plant. 105*, 585−592.
27. Ruben, S., Randall, M., Kamen, M. D., and Hyde, J. L. (1941) Heavy oxygen (^{18}O) as a tracer in the study of photosynthesis, *J. Am. Chem. Soc. 63*, 877−879.
28. Kamen, M. D., and Barker, H. A. (1945) Inadequacies in the present knowledge of the relation between photosynthesis and the ^{18}O content of atmospheric oxygen, *Proc. Natl. Acad. Sci. U.S.A. 31*, 8−15.
29. Warburg, O., and Krippahl, G. (1958) Hill-Reaktionen, *Z. Naturforsch., B: Chem. Sci. 13*, 509−514.
30. Warburg, O., and Krippahl, G. (1960) Notwendigkeit der kohlensaure fur die chinonreaktionen und ferricyanidreaktionen in grunen grana, *Z. Naturforsch. B: Chem. Sci. 15*, 367−369.
31. Dole, M., and Jenks, G. (1944) Isotopic composition of photosynthetic oxygen, *Science 100*, 409.
32. Stevens, C. L. R., Schultz, D., Vanbaalen, C., and Parker, P. L. (1975) Oxygen isotope fractionation during photosynthesis in a blue-green and a green alga, *Plant Physiol. 56*, 126−129.
33. Metzner, H., Fischer, K., and Bazlen, O. (1981) The precursor of the photosynthetic oxygen, in *Photosynthesis II: Electron Transport and Photophosphorylation* (Akoyunoglou, G., Ed.) pp 375−387, Balaban International Science Services, Philadelphia, PA.
34. Lu, Y. K., and Stemler, A. J. (2002) Extrinsic photosystem II carbonic anhydrase in maize mesophyll chloroplasts, *Plant Physiol. 128*, 643−649.
35. Villarejo, A., Shutova, T., Moskvin, O., Forssen, M., Klimov, V. V., and Samuelsson, G. (2002) A photosystem II-associated carbonic anhydrase regulates the efficiency of photosynthetic oxygen evolution, *EMBO J. 21*, 1930−1938.
36. Moskvin, O. V., Shutova, T. V., Khristin, M. S., Ignatova, L. K., Villarejo, A., Samuelsson, G., Klimov, V. V., and Ivanov, B. N. (2004) Carbonic anhydrase activities in pea thylakoids—A photosystem II core complex-associated carbonic anhydrase. *Photosynth. Res. 79*, 93−100.
37. Stemler, A., and Radmer, R. (1975) Source of photosynthetic oxygen in bicarbonate-stimulated Hill reaction, *Science 190*, 457−458.
38. Radmer, R., and Ollinger, O. (1980) Isotopic composition of photosynthetic O_2 flash yields in the presence of $H_2{}^{18}O$ and $HC^{18}O_3^-$, *FEBS Lett. 110*, 57−61.
39. Guy, R. D., Fogel, M. L., and Berry, J. A. (1993) Photosynthetic fractionation of the stable isotopes of oxygen and carbon, *Plant Physiol. 101*, 37−47.
40. Helman, Y., Barkan, E., Eisenstadt, D., Luz, B., and Kaplan, A. (2005) Fractionation of the three stable oxygen isotopes by oxygen-producing and oxygen-consuming reactions in photosynthetic organisms, *Plant Physiol. 138*, 2292−2298.
41. Radmer, R., and Ollinger, O. (1986) Do the higher oxidation states of the photosynthetic O_2-evolving system contain bound water? *FEBS Lett. 195*, 285−289.
42. Messinger, J., Badger, M., and Wydrzynski, T. (1995) Detection of *one* slowly exchanging substrate water molecule in the S_3 state of photosystem II, *Proc. Natl. Acad. Sci. U.S.A. 92*, 3209−3213.
43. Hillier, W., Messinger, J., and Wydrzynski, T. (1998) Kinetic determination of the fast exchanging substrate water molecule in the S_3 state of photosystem II, *Biochemistry 37*, 16908−16914.
44. Hillier, W., and Wydrzynski, T. (2001) Oxygen ligand exchange at metal sites: Implications for the O_2 evolving mechanism of photosystem II, *Biochim. Biophys. Acta 1503*, 197−209.
45. Clausen, J., Beckmann, K., Junge, W., and Messinger, J. (2005) Evidence that bicarbonate is not the substrate in photosynthetic oxygen evolution, *Plant Physiol. 139*, 1444−1450.
46. Hillier, W., McConnell, I., Boussac, A., Messinger, J., Badger, M. R., Dismukes, G. C., and Wydrzynski, T. (2004) in *Photosynthesis: Fundamental Aspects to Global Perspectives* (Van der Est, A., and Bruce, D., Eds.) pp 293−296, Allen Press Inc., Lawrence, Kansas, Montàeal.
47. Berthold, D. A., Babcock, G. T., and Yocum, C. F. (1981) A highly resolved, oxygen-evolving photosystem II preparation from spinach thylakoid membranes, *FEBS Lett. 134*, 231−234.
48. Boussac, A., Rappaport, F., Carrier, P., Verbavatz, J. M., Gobin, R., Kirilovsky, D., Rutherford, A. W., and Sugiura, M. (2004) Biosynthetic Ca^{2+}/Sr^{2+} exchange in the photosystem II oxygen-evolving enzyme of *Thermosynechococcus elongatus*, *J. Biol. Chem. 279*, 22809−22819.
49. Billo, E. J. (2001) *Excel for Chemists: A Comprehensive Guide*, 2nd ed., Wiley-VCH, New York.
50. de Levie, R. (1999) Estimating parameter precision in nonlinear least squares with excel's solver, *J. Chem. Educ. 76*, 1594−1598.
51. Salter, C. (2000) Error analysis using the variance-covariance matrix, *J. Chem. Educ. 77*, 1239−1243.
52. Ananyev, G., and Dismukes, G. C. (2005) How fast can photosystem II split water? Kinetic performance at high and low frequencies, *Photosynth. Res. 84*, 355−365.
53. Mills, G. A., and Urey, H. C. (1940) The kinetics of isotopic exchange between carbon dioxide, bicarbonate ion, carbonate ion and water, *J. Am. Chem. Soc. 62*, 1019−1026.
54. Lindskog, S., and Coleman, J. E. (1973) Catalytic mechanism of carbonic-anhydrase, *Proc. Natl. Acad. Sci. U.S.A. 70*, 2505−2508.
55. Silverman, D. N. (1982) Carbonic anhydrase: Oxygen-18 exchange catalyzed by an enzyme with rate-contributing proton-transfer steps, *Methods Enzymol. 87*, 732−752.
56. Badger, M. R., and Price, G. D. (1989) Carbonic-anhydrase activity associated with the cyanobacterium Synechococcus PCC7942, *Plant Physiol. 89*, 51−60.
57. Gerster, R. (1971) Kinetics of oxygen exchange between gaseous $C^{18}O_2$ and water, *Int. J. Appl. Radiat. Isot. 22*, 339−348.
58. Tu, C. K., and Silverman, D. N. (1975) Kinetics of exchange of oxygen between carbon-dioxide and carbonate in aqueous-solution, *J. Phys. Chem. 79*, 1647−1651.
59. Magid, E., and Turbeck, B. O. (1968) Rates of spontaneous hydration of CO_2 and reciprocal reaction in neutral aqueous solutions between 0 degrees and 38 degrees, *Biochim. Biophys. Acta 165*, 515.
60. Gibbons, B. H., and Edsall, J. T. (1963) Rate of hydration of carbon dioxide and dehydration of carbonic acid at 25 degrees, *J. Biol. Chem. 238*, 3502.
61. Nier, A. O. (1950) A redetermination of the relative abundances of the isotopes of carbon, nitrogen, oxygen, argon, and potassium, *Phys. Rev. 77*, 789−793.
62. Metzner, H. (1975) Water decomposition in photosynthesis—Critical reconsideration, *J. Theor. Biol. 51*, 201−231.
63. Loll, B., Kern, J., Saenger, W., Zouni, A., and Biesiadka, J. (2005) Towards complete cofactor arrangement in the 3.0Å resolution structure of photosystem II, *Nature 438*, 1040−1044.

BI051892O